

# Polarized top decay into polarized $W$ $t(\uparrow) \rightarrow W(\uparrow) + b$ at $O(\alpha_s)$

M. Fischer, S. Groote, J.G. Körner and M.C. Mauser

Institut für Physik, Johannes-Gutenberg-Universität  
Staudinger Weg 7, D-55099 Mainz, Germany

and

B. Lampe

Sektion Physik  
Ludwig-Maximilians-Universität München  
Theresienstraße 37, D-80333 München

and

MPI für Physik, Werner-Heisenberg-Institut  
Föhringer Ring 6, D-80805 München

## Abstract

We consider the decay of a polarized top quark into a polarized  $W$ -boson plus a bottom quark, followed by the decay of the  $W$ -boson into a pair of leptons or quarks. The polar angle distribution of the top spin relative to the  $W$ -momentum and the polar angle distribution of the lepton (or quark) in the  $W$ -rest frame is governed by three polarized and three unpolarized rate functions which are related to the double density matrix elements of the decay  $t \rightarrow W^+ + b$ . We obtain analytical expressions for the  $O(\alpha_s)$  radiative corrections to the three polarized and three unpolarized rate functions. We also provide a comprehensive discussion of the dependence of the longitudinal, transverse and normal polarization of the top quarks produced at  $e^+e^-$ -colliders on beam polarization parameters.

It is well-known that quarks produced in  $e^+e^-$ -annihilation possess a high degree of polarization. This holds true for the production of light quarks ( $u, d, s, c, b$ ) as well as for heavy top quarks. The top quark is very short-lived and therefore retains its full polarization content when it decays. By measuring the momenta and spin orientation of its decay products one can then define spin-momentum and spin-spin correlations between the top quark spin and its decay products which will allow for detailed studies of the top decay mechanism.

In this paper we study momentum and spin-momentum correlations in the cascade decay process  $t \rightarrow W^+ + b$  followed by  $W^+ \rightarrow l^+ + \nu_l$  or  $W \rightarrow \bar{q} + q$ . The step-one decay  $t \rightarrow W^+ + b$  is analyzed in the  $t$ -rest frame where we study the spin-momentum correlation between the spin of the top and the momentum of the  $W$ . In step two we go to the rest frame of the  $W$  and analyze the correlation between the momentum of the lepton (or antiquark) and the initial momentum of the  $W$ , i.e. we thereby analyze the spin density matrix of the  $W$ .

One of the attractions of the envisaged future high energy linear colliders is the possibility to tune the polarization of the top quark over a wide range of polarization values by making use of the possibility of linear colliders to polarize their  $e^+$  and  $e^-$  beams. Prospective linear  $e^+e^-$ -colliders are planned to have available maximal polarizations of  $P(e^-) = 80-90\%$  and  $P(e^+) = 60-70\%$ .

Before we turn to the main subject of the paper, namely the decay of a polarized top quark into a polarized  $W$  and a (massless) bottom quark, we want to first demonstrate the capabilities of linear colliders to tune the polarization of the top quarks through the use of beam polarization. To this end we write down the functional dependence of the mean longitudinal and transverse components of the top quark's polarization on the beam polarization parameters. Here the mean refers to polar angle averaging over the polar angle between the beam and the top quark. In the Standard Model and at the Born term level one has (see e.g. [1-4])

$$P^L = \frac{4}{3} \frac{[h_1 g_{14} + h_2 g_{44}]v}{[h_1 g_{11} + h_2 g_{41}](1 + \frac{1}{3}v^2) + [h_1 g_{12} + h_2 g_{42}](1 - v^2)} \quad (1)$$

and

$$P^\perp = -\frac{\pi}{2} \frac{m_t}{\sqrt{q^2}} \frac{h_2(g_{11} + g_{12}) + h_1(g_{41} + g_{42})}{[h_1 g_{11} + h_2 g_{41}](1 + \frac{1}{3}v^2) + [h_1 g_{12} + h_2 g_{42}](1 - v^2)} \quad (2)$$

where  $v = (1 - 4m^2/q^2)^{1/2}$ ,  $h_1 = 1 - h^- h^+$ ,  $h_2 = h^- - h^+$  and  $h^-$  and  $h^+$  are the longitudinal (or helicity) polarizations of the  $e^-$  and  $e^+$  beams, respectively. The electroweak model dependence is specified by the electroweak model parameters  $g_{ij}$  which, in the Standard Model, read [3]

$$g_{11} = \frac{4}{9} - \frac{4}{3} v_e v_t \operatorname{Re}(\chi_Z) + (v_e^2 + a_e^2)(v_t^2 + a_t^2) |\chi_Z|^2 \quad (3)$$

$$g_{12} = \frac{4}{9} - \frac{4}{3} v_e v_t \operatorname{Re}(\chi_Z) + (v_e^2 + a_e^2)(v_t^2 - a_t^2) |\chi_Z|^2 \quad (4)$$

$$g_{14} = \frac{4}{3} v_e a_t \operatorname{Re}(\chi_Z) - 2(v_e^2 + a_e^2) v_t a_t |\chi_Z|^2 \quad (5)$$

$$g_{41} = \frac{4}{3} a_e v_t \operatorname{Re}(\chi_Z) - 2(v_t^2 + a_t^2) v_e a_e |\chi_Z|^2 \quad (6)$$

$$g_{42} = \frac{4}{3} a_e v_t \operatorname{Re}(\chi_Z) - 2(v_t^2 - a_t^2) v_e a_e |\chi_Z|^2 \quad (7)$$

$$g_{44} = -\frac{4}{3} a_e a_t \operatorname{Re}(\chi_z) + 4 v_e a_e v_t a_t |\chi_Z|^2 \quad (8)$$

$$v_e = -1 + 4 \sin^2 \theta_W, \quad a_e = -1, \quad v_t = 1 - \frac{8}{3} \sin^2 \theta_W, \quad a_t = 1 \quad (9)$$

and where the propagator function  $\chi_Z$  reads

$$\chi_Z(s) = g M_Z^2 \frac{s}{s - M_Z^2 + i M_Z \Gamma_Z}. \quad (10)$$

$M_Z$  and  $\Gamma_Z$  are the mass and width of the Z-boson and  $g = G_F(8\sqrt{2}\pi\alpha)^{-1} \approx 4.49 \cdot 10^{-5} \text{ GeV}^{-2}$ . We take  $\sin^2 \theta_W = 0.23124$  from [20].

At the Born term level the polarization lies entirely in the plane spanned by the beam and the top quark (we are neglecting an imaginary contribution from the Breit-Wigner form of the propagator function). In Fig. 1 we plot the two non-vanishing components of the top polarization  $P^L$  and  $P^\perp$  as a function of the center of mass energy  $\sqrt{q^2}$  for  $h^+ = 0$ , and  $h^-$  ranges from  $-1$  to  $+1$  in increments of  $0.2$ . The boundary curves  $h^- = -1$  and  $h^- = +1$  for both the longitudinal and transverse polarization can be seen to be independent of the value of  $h^+$ . At  $\sqrt{q^2} = 500 \text{ GeV}$  the longitudinal polarization becomes as large as  $P^L = -52.2\%$  and  $P^L = +65.2\%$  for  $h^- = -1$  and  $h^- = +1$ , respectively. The value of  $h^+$  determines the density of the  $h^-$ -lines as the region between the two boundary curves is traversed. For  $h^+ \approx -0.3$  the different  $h^-$ -lines become approximately equally spaced. For  $h^+ \rightarrow -1$  the different  $h^-$ -lines migrate towards the upper boundary curve  $h^- = +1$ , whereas they migrate towards the lower boundary curve  $h^- = -1$  for  $h^+ \rightarrow +1$ .

The case  $h^+ = 0$  depicted in Fig. 1 provides a good demonstration of the possibilities of polarization tuning at  $e^+e^-$ -colliders. In addition it does not require the positron beam to be polarized which is an advantage. The transverse polarization shown in Fig. 1 is generally comparable in size to the longitudinal polarization. At  $\sqrt{q^2} = 500 \text{ GeV}$  the transverse polarization is  $P^\perp = -1.8\%$  and  $P^\perp = -2.2\%$  for  $h^- = -1$  and  $h^- = +1$ , respectively. It shows the expected  $1/\sqrt{q^2}$  fall-off behaviour while the longitudinal polarization slightly increases with energy. We want to remind the reader that we have calculated the mean polarization of the top after averaging over the relative orientation between the beam and the top quark. In fact, the  $\cos \theta$ -dependence of the polarization can be quite strong in particular for small values of the mean polarization [1–4].

The  $O(\alpha_s)$  radiative corrections to the Born term polarization have been calculated in [3–6]. They are generally quite small. Also at  $O(\alpha_s)$  a small polarization

contribution normal to the beam-event plane comes in through the imaginary part of the one-loop contribution [1, 4]. For the normal polarization  $P^N$  one obtains<sup>1</sup> [1, 4]

$$P^N = -\frac{\pi}{6} \frac{m_t}{\sqrt{q^2}} (2-v^2) \alpha_s \frac{h_2 g_{14} + h_1 g_{44}}{[h_1 g_{11} + h_2 g_{41}] (1 + \frac{1}{3} v^2) + [h_1 g_{12} + h_2 g_{42}] (1 - v^2)}. \quad (11)$$

In Fig. 2 we plot the normal component of the top polarization  $P^N$  as a function of the center of mass energy again for  $h^+ = 0$ , where  $h^-$  ranges from  $h^- = -1$  to  $h^+ = 1$  in increments of 1. As before the boundary curves for  $h^- = -1$  and  $h^- = 1$  are independent of  $h^+$  as a simple inspection of Eq. (11) shows. Contrary to e.g.  $P^L$  in Eq. (1) the numerator in Eq. (11) determining  $P^N$  for the two boundary curves is now given by  $\pm(g_{14} \pm g_{44})$  and not by  $(g_{14} \pm g_{44})$ . From the values of  $g_{14}$  and  $g_{44}$  this implies that the boundary curves for  $P^N$  are not as spread apart as for  $P^L$ . The numerical value of  $P^N$  is generally quite small which, in part, is due to the overall factor  $\alpha_s$  multiplying  $P^N$ . The normal component  $P^N$  shows the expected  $1/\sqrt{q^2}$  fall-off behaviour.

We now turn to the main subject of this paper, namely the decay of a polarized top quark into an on-shell polarized  $W^+$  and a massless bottom quark. The polarization of the  $W^+$  can be probed through the angular decay distribution of its decay products, which can be a lepton pair ( $l^+, \nu_l$ ) or a light quark-antiquark pair. In Fig.2 we introduce the two polar angles  $\theta_P$  and  $\theta$ . They are defined in the two respective rest frames of the two-step cascade process  $t \rightarrow W^+ + b$  followed by  $W^+ \rightarrow l^+ + \nu_l$  or  $W^+ \rightarrow \bar{q} + q$ . The double polar angle decay distribution is given by (see e.g. [7])

$$\begin{aligned} \frac{1}{\Gamma_0} \frac{d\Gamma}{d \cos \theta_P d \cos \theta} &= \frac{1}{2} \left( \hat{\Gamma}_U + \hat{\Gamma}_U^P P \cos \theta_P \right) \frac{3}{8} \left( 1 + \cos^2 \theta \right) \\ &+ \frac{1}{2} \left( \hat{\Gamma}_L + \hat{\Gamma}_L^P P \cos \theta_P \right) \frac{3}{4} \sin^2 \theta \\ &+ \frac{1}{2} \left( \hat{\Gamma}_F + \hat{\Gamma}_F^P P \cos \theta_P \right) \frac{3}{4} \cos \theta. \end{aligned} \quad (12)$$

As a reference rate we take the total Born term rate  $\Gamma_0 = \Gamma_{U+L}(\text{Born})$  given by ( $x = m_W/m_t$ )

$$\Gamma_0 = \frac{G_F m_W^2 m_t}{4\sqrt{2}\pi} |V_{tb}|^2 \frac{(1-x^2)^2 (1+2x^2)}{x^2}. \quad (13)$$

We have defined scaled rate functions  $\hat{\Gamma}_i$  and  $\hat{\Gamma}_i^P$  according to  $\hat{\Gamma}_i = \Gamma_i/\Gamma_0$  and  $\hat{\Gamma}_i^P = \Gamma_i^P/\Gamma_0$ . The subscripts in the unpolarized rate functions  $\Gamma_i$  and the polarized rate functions  $\Gamma_i^P$  ( $i=U, L, F$ ) refer to three measurable polarization states of the  $W^+$  ( $U$ : unpolarized transverse;  $L$ : longitudinal;  $F$ : forward-backward asymmetric). For example, for the unpolarized rate functions  $\Gamma_i$  ( $i=U, L, F$ ) the three

<sup>1</sup>There is a factor  $(v_e^2 + a_e^2)^{-1}$  missing on the r.h.s of Eq.(16) in [1].

components are determined by the three linear combinations  $\Gamma_U = \Gamma_{++} + \Gamma_{--}$ ,  $\Gamma_L = \Gamma_{00}$  and  $\Gamma_F = \Gamma_{++} - \Gamma_{--}$  of the diagonal density matrix elements  $\Gamma_{\lambda_W, \lambda_W}$  of the  $W$  ( $\lambda_W = \lambda'_W = 0, \pm 1$ ), and similarly for the polarized rate functions. The total rate is obviously given by  $\Gamma = \Gamma_U + \Gamma_L := \Gamma_{U+L}$  as is evident from Eq. (12) after  $\cos\theta$  and  $\cos\theta_P$  integration. For the unpolarized rate functions one sums over the two diagonal density matrix elements of the top quark whereas one takes the difference of the two for the polarized rate functions. In practise this is achieved by replacing the spin sum  $(\not{p}_t + m_t)$  by  $(\not{p}_t + m_t)\gamma_5 \not{s}_t$  when calculating the polarized rate functions, where  $s_t^\mu = (0, 0, 0, 1)$  in the rest frame of the top quark.

Let us first list the Born term contributions to the rate functions. They are given by

$$\begin{aligned} \hat{\Gamma}_U(\text{Born}) &= \frac{2x^2}{1+2x^2} & \hat{\Gamma}_U^P(\text{Born}) &= \frac{-2x^2}{1+2x^2} \\ \hat{\Gamma}_L(\text{Born}) &= \frac{1}{1+2x^2} & \hat{\Gamma}_L^P(\text{Born}) &= \frac{1}{1+2x^2} \\ \hat{\Gamma}_F(\text{Born}) &= \frac{-2x^2}{1+2x^2} & \hat{\Gamma}_F^P(\text{Born}) &= \frac{2x^2}{1+2x^2} \end{aligned} \quad (14)$$

The reason that one has  $\hat{\Gamma}_U = -\hat{\Gamma}_F = -\hat{\Gamma}_U^P = \hat{\Gamma}_F^P$  and  $\hat{\Gamma}_L = \hat{\Gamma}_L^P$  at the Born term level is that, with a massless  $b$ -quark and a  $(V-A)$  interaction, only the two helicity configurations ( $\lambda_t = -1/2; \lambda_W = -1$ ) and ( $\lambda_t = 1/2; \lambda_W = 0$ ) can be realized. For antitop decay one has the two helicity configurations ( $\lambda_{\bar{t}} = 1/2; \lambda_W = 1$ ) and ( $\lambda_{\bar{t}} = -1/2; \lambda_W = 0$ ) such that  $\hat{\Gamma}_U^P \rightarrow -\hat{\Gamma}_U^P$ ,  $\hat{\Gamma}_L^P \rightarrow -\hat{\Gamma}_L^P$ ,  $\hat{\Gamma}_F \rightarrow -\hat{\Gamma}_F$ , while the other rate functions remain unchanged.

The  $O(\alpha_s)$  radiative corrections to the Born term contributions are determined by the sum of the one-loop contributions and the tree-graph contributions. Each of the two classes of contributions are infrared (IR) and mass (M) singular but the singularities cancel in the sum. As a regularization procedure for the regularization of the IR/M singularities we have chosen to endow the gluon and the bottom quark with (small) masses  $m_g$  and  $m_b$ . We have given preference to mass regularization over dimensional regularization because we wanted to circumvent the notorious  $\gamma_5$  problem in dimensional regularization which comes in for the polarization observables calculated in this paper. The IR/M singularities show up as powers of logarithms (up to second order) of the mass regulators. The logarithmic contributions cancel in the sum of the one-loop and tree-graph contributions and one remains with a finite result. All of this is by now standard procedure and we shall not dwell on the subject of IR/M regularization any further. The details of the calculation will be presented in a forthcoming publication. We reiterate that our results are given for  $m_b = 0$ . We expect that the  $m_b \neq 0$  corrections are of the same size as in the Born term contributions where they amount to 0.17% in the total rate.

Including the Born term contributions the full  $O(\alpha_s)$  results are given by

$$\begin{aligned}
\hat{\Gamma}_U &= \frac{2x^2}{1+2x^2} + \frac{\alpha_s}{2\pi} C_F \frac{x^2}{(1-x^2)^2(1+2x^2)} \left\{ (x^2-1)(19+x^2) + \frac{2}{3}\pi^2(5+5x^2-2x^4) \right. \\
&\quad - 2\frac{(1-x^2)^2(1+2x^2)}{x^2} \ln(1-x^2) - 4(5+7x^2-2x^4) \ln(x) - 2\frac{(1-x)^2(5+7x^2+4x^3)}{x} \\
&\quad \times \ln(x) \ln(1-x) + 2\frac{(1+x)^2(5+7x^2-4x^3)}{x} \ln(x) \ln(1+x) - (5+4x+15x^2+8x^3) \\
&\quad \left. \times 2\frac{(1-x)^2}{x} \text{Li}_2(x) + 2\frac{(1+x)^2(5-4x+15x^2-8x^3)}{x} \text{Li}_2(-x) \right\} \quad (15)
\end{aligned}$$

$$\begin{aligned}
\hat{\Gamma}_L &= \frac{1}{1+2x^2} + \frac{\alpha_s}{2\pi} C_F \frac{x^2}{(1-x^2)^2(1+2x^2)} \left\{ \frac{(1-x^2)(5+47x^2-4x^4)}{2x^2} - \frac{2}{3}\pi^2 \times \right. \\
&\quad \times \frac{(1+5x^2+2x^4)}{x^2} - \frac{3(1-x^2)^2}{x^2} \ln(1-x^2) + 16(1+2x^2) \ln(x) - (2-x+6x^2+x^3) \\
&\quad \times 2\frac{(1-x)^2}{x^2} \ln(1-x) \ln(x) - 2\frac{(1+x)^2(2+x+6x^2-x^3)}{x^2} \ln(x) \ln(1+x) \\
&\quad \left. - 2\frac{(1-x)^2(4+3x+8x^2+x^3)}{x^2} \text{Li}_2(x) - 2\frac{(1+x)^2(4-3x+8x^2-x^3)}{x^2} \text{Li}_2(-x) \right\} \quad (16)
\end{aligned}$$

$$\begin{aligned}
\hat{\Gamma}_F &= \frac{-2x^2}{1+2x^2} + \frac{\alpha_s}{2\pi} C_F \frac{x^2}{(1-x^2)^2(1+2x^2)} \left\{ 2(1-x)^2(4x-3) + \frac{2}{3}\pi^2(2+x^2) \right. \\
&\quad + 2\frac{(1-x^2)^2(1+2x^2)}{x^2} \ln(1-x) + 2\frac{(1-x^2)(1-9x^2+2x^4)}{x^2} \ln(1+x) \\
&\quad \left. + 8(1-x^2)^2 \text{Li}_2(x) + 8(1+3x^2-x^4) \text{Li}_2(-x) \right\} \quad (17)
\end{aligned}$$

$$\begin{aligned}
\hat{\Gamma}_U^P &= \frac{-2x^2}{1+2x^2} + \frac{\alpha_s}{2\pi} C_F \frac{x^2}{(1-x^2)^2(1+2x^2)} \left\{ \frac{(1-x)^2(-12+55x-6x^2+x^3)}{x} - \frac{10}{3}\pi^2 \times \right. \\
&\quad \times (2+x^2) + 2\frac{(1-x^2)^2(1+2x^2)}{x^2} \ln(1-x) + 2\frac{(1-x^2)(7+21x^2+2x^4)}{x^2} \ln(1+x) \\
&\quad \left. + 8(1-x^2)^2 \text{Li}_2(x) - 8(11+3x^2+x^4) \text{Li}_2(-x) \right\} \quad (18)
\end{aligned}$$

$$\begin{aligned}
\hat{\Gamma}_L^P &= \frac{1}{1+2x^2} + \frac{\alpha_s}{2\pi} C_F \frac{x^2}{(1-x^2)^2(1+2x^2)} \left\{ - (15-22x+105x^2-24x^3+4x^4) \times \right. \\
&\quad \times \frac{(1-x)^2}{2x^2} + \frac{1}{3}\pi^2 \frac{(1+24x^2+10x^4)}{x^2} - 3\frac{(1-x^2)^2}{x^2} \ln(1-x) - \frac{(1-x^2)(17+53x^2)}{x^2} \times \\
&\quad \left. \times \ln(1+x) - 4\frac{(1-x^2)^2}{x^2} \text{Li}_2(x) + 4\frac{(2+22x^2+11x^4)}{x^2} \text{Li}_2(-x) \right\} \quad (19)
\end{aligned}$$

$$\begin{aligned}
\hat{\Gamma}_F^P = & \frac{2x^2}{1+2x^2} + \frac{\alpha_s}{2\pi} C_F \frac{x^2}{(1-x^2)^2(1+2x^2)} \left\{ 2(1-x^2)(4+x^2) - \frac{2}{3}\pi^2(1+x^2+2x^4) \right. \\
& - 2\frac{(1-x^2)^2(1+2x^2)}{x^2} \ln(1-x^2) - 4(2-5x^2-2x^4) \ln(x) - \ln(x) \ln(1-x) \times \\
& \times 4\frac{(1-x)^2(1+3x+2x^2+2x^3)}{x} + 4\frac{(1+x)^2(1-3x+2x^2-2x^3)}{x} \ln(x) \ln(1+x) \\
& \left. - 4\frac{(1-x)^2(1+5x+6x^2+4x^3)}{x} \text{Li}_2(x) + 4\frac{(1+x)^2(1-5x+6x^2-4x^3)}{x} \text{Li}_2(-x) \right\} \quad (20)
\end{aligned}$$

Analytical results have been given before on the total rate  $\Gamma_{U+L}$  [8–10]<sup>2</sup> and on the ratio  $\Gamma_U/\Gamma_L$  [12]. We find full agreement with these results. Our analytical results on  $\Gamma_F$  and the polarized rate functions  $\Gamma_i^P$  are new. We have also compared our results with the numerical results on the remaining rate functions given in [13, 14]. Again we find agreement.

We now discuss our numerical results. The strong coupling constant has been evolved from the  $M_Z$ -scale ( $\alpha_s(M_Z) = 0.1175$ ) to the top quark mass scale. Thus we take  $\alpha_s(m_t = 175 \text{ GeV}) = 0.10702$  with  $m_W = 80.22 \text{ GeV}$ . The numerical values for the Born term and the  $O(\alpha_s)$  corrections are given by

$$\begin{aligned}
\hat{\Gamma}_U = & 0.296(1 - 0.062) & \hat{\Gamma}_U^P = & -0.296(1 - 0.069) \\
\hat{\Gamma}_L = & 0.704(1 - 0.095) & \hat{\Gamma}_L^P = & 0.704(1 - 0.096) \\
\hat{\Gamma}_F = & -0.296(1 - 0.069) & \hat{\Gamma}_F^P = & 0.296(1 - 0.064).
\end{aligned} \quad (21)$$

The radiative corrections to the unpolarized and polarized rate functions are sizeable and range from 6.2% to 9.6%. However, the radiative corrections all go in the same direction. This is an indication that the main contributions to the radiative corrections come from the tree-diagrams from phase-space regions close to the IR/M singularities. Similar observations have been made for the radiative corrections to polarization-type structure functions in other production or decay processes. When forming ratios of the rate functions, as is appropriate for the definition of polarization-type observables, the size of the radiative corrections to the polarization-type observables are much reduced. For example, the  $O(\alpha_s)$  radiative corrections to the ratio  $\Gamma_U/\Gamma_L$  and  $\Gamma_F/\Gamma_{U+L}$  are reduced to 3.65% and 1.77%, respectively.

In conclusion, we have obtained analytical results on the  $O(\alpha_s)$  corrections to the six unpolarized and polarized rate functions that describe the double polar angle distribution of the decay of a polarized top quark into a  $W$  and a massless  $b$ -quark followed by the decay of the  $W$  into a lepton pair or a quark pair. For antitop decay one has to change the signs of the three rate functions  $\hat{\Gamma}_U^P$ ,  $\hat{\Gamma}_L^P$  and  $\hat{\Gamma}_F$ . There are two more rate functions in the decay that were not discussed in this paper. They describe the relative azimuthal angle dependence of the

---

<sup>2</sup>The total rate also follows from the work of [11]

two decay planes that can be defined in the two-step decay process. Results on these additional azimuthal rate functions will be presented in a forthcoming publication.

We have also provided a comprehensive discussion of the polarization of top quarks produced in  $e^+e^-$ -annihilation having the production of top quark pairs at future linear  $e^+e^-$ -colliders in mind. As concerns polarized top decay, there are of course other areas of application of our decay analysis. For example, polarized top quarks are also produced in single top quark production at hadron colliders [15]. Further, there is a high degree of correlation between the polarization of top and anti-top quarks produced in pairs either at  $e^+e^-$  [16–18] or hadron colliders [19] which can be probed through the joint decay distributions of the top and the anti-top.

**Acknowledgements:** M. Fischer and M.C. Mauser were supported by the DFG (Germany) through the Graduiertenkolleg „Teilchenphysik bei hohen und mittleren Energien“ at the University of Mainz. S. Groote and J.G. Körner acknowledge partial support by the BMBF (Germany) under contract 06MZ865.

## References

- [1] J.H. Kühn, A. Reiter and P. Zerwas, Nucl. Phys. **B272** (1986) 560
- [2] M. Anselmino, P. Kroll and B. Pire, Phys. Lett. **B167** (1986) 113
- [3] S. Groote, J.G. Körner and M.M. Tung, Z. Phys. **C74** (1997) 615
- [4] S. Groote and J.G. Körner, Z. Phys. **C74** (1996) 255
- [5] J.G. Körner, A. Pilaftsis and M.M. Tung, Z. Phys. **C63** (1994) 575
- [6] S. Groote, J.G. Körner and M.M. Tung, Z. Phys. **C70** (1996) 281
- [7] P. Bialas, J.G. Körner, M. Krämer and K. Zalewski, Z. Phys. **C57** (1993) 115
- [8] J. Liu and Y.-P. Yao, Int. J. Mod. Phys. **A6** (1991) 4925
- [9] A. Czarnecki, Phys. Lett. **B252** (1990) 467
- [10] C.S. Li, R.J. Oakes and T.C. Yuan, Phys. Rev. **D43** (1991) 3759
- [11] M. Jezabek and J.H. Kühn, Nucl. Phys. **B314** (1989) 1
- [12] B. Lampe, Nucl. Phys. **B458** (1996) 23
- [13] B. Lampe, Nucl. Phys. **B454** (1995) 506

- [14] B. Lampe, Complete Description of Polarization Effects in Top Quark Decays Including Higher Order QCD Corrections, Report No. MPI-PHT-98-07(1997)26, e-Print Archive: hep-ph/9801346
- [15] G. Mahlon and S. Parke, Phys. Rev. **D55** (1997) 7249
- [16] S. Parke and Y. Shadmi, Phys. Lett. **B387** (1996) 199
- [17] M. M. Tung, J. Bernabéu and J. Peñarrocha, Phys. Lett. **B418** (1998) 181  
S. Groote, J. G. Körner and A. J. Leyva, Phys. Lett. **B418** (1998) 192
- [18] A. Brandenburg, M. Flesch and P. Uwer, Phys. Rev. **D59** (1999) 014001
- [19] G. Mahlon and S. Parke, Phys. Rev. **D53** (1996) 4886, Phys. Lett. **B411** (1997) 173
- [20] Particle Data Group, Eur. Phys. J. **C3** (1998) 1

## Figure Captions

- Fig. 1:** Examples of polarization tuning of the top quark at  $e^+e^-$ - colliders through changes of the beam polarization with  $h^+ = 0$  and  $h^-$  ranging from  $-1$  to  $+1$  in steps of  $\Delta h^- = 0.2$ .
- Fig. 2:** Normal component  $P^N$  of top polarization at  $O(\alpha_s)$ . Shown are polarization values for  $h^+ = 0$  ranging from  $h^- = -1$  to  $h^- = 1$  in steps of  $\Delta h^- = 1$ .
- Fig. 3:** Definition of the polar angles  $\theta_P$  and  $\theta$  in the top and in the  $W^+$  rest frame, respectively.

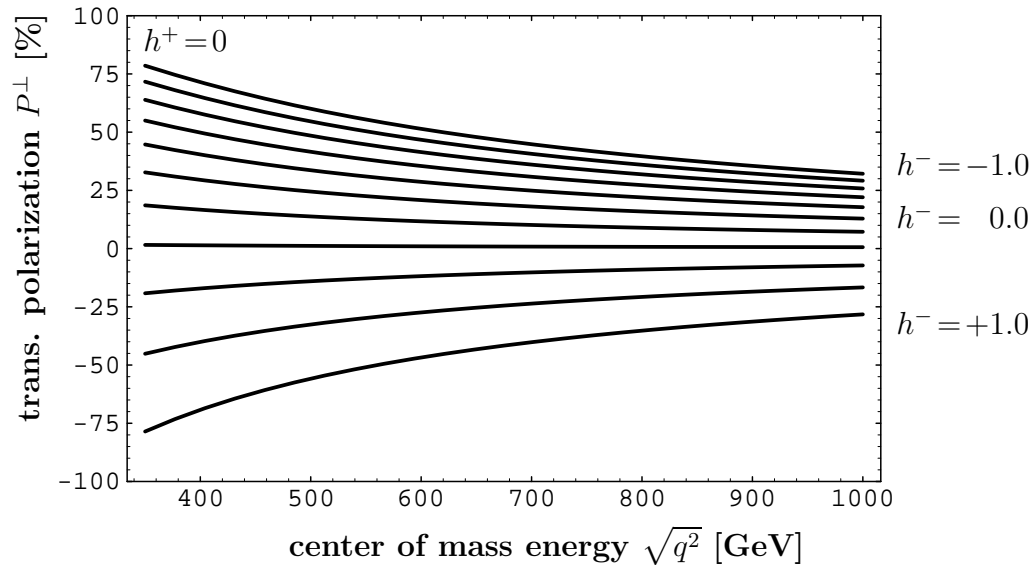
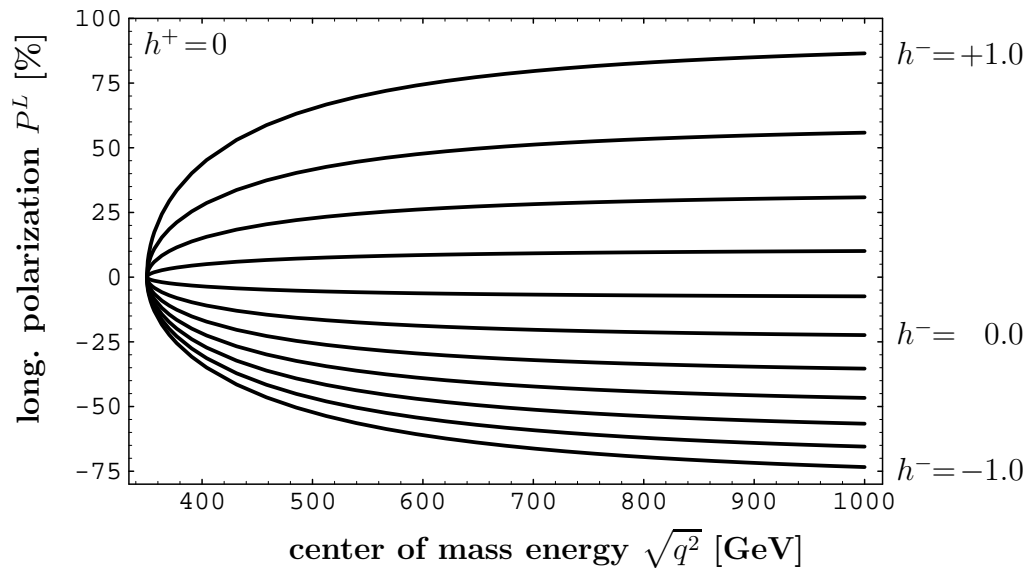
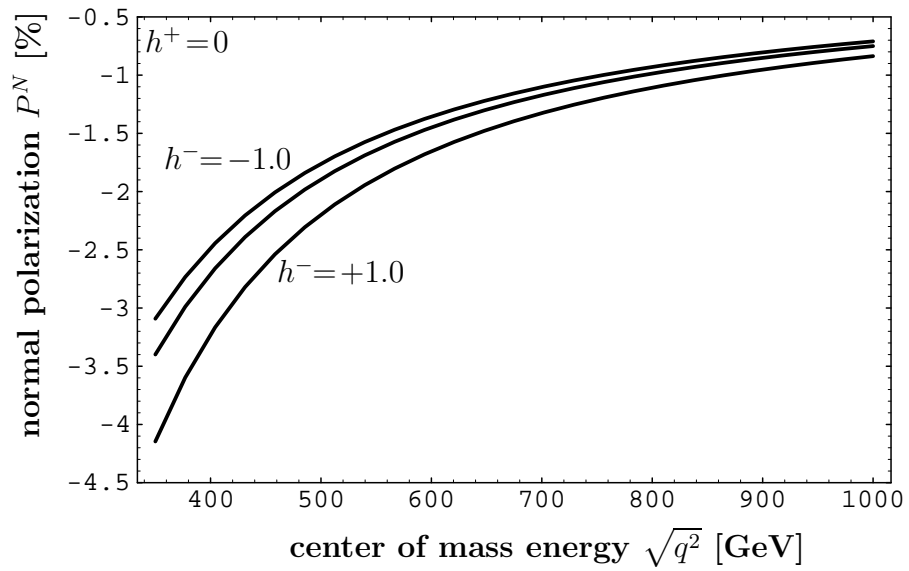


Figure 1



**Figure 2**

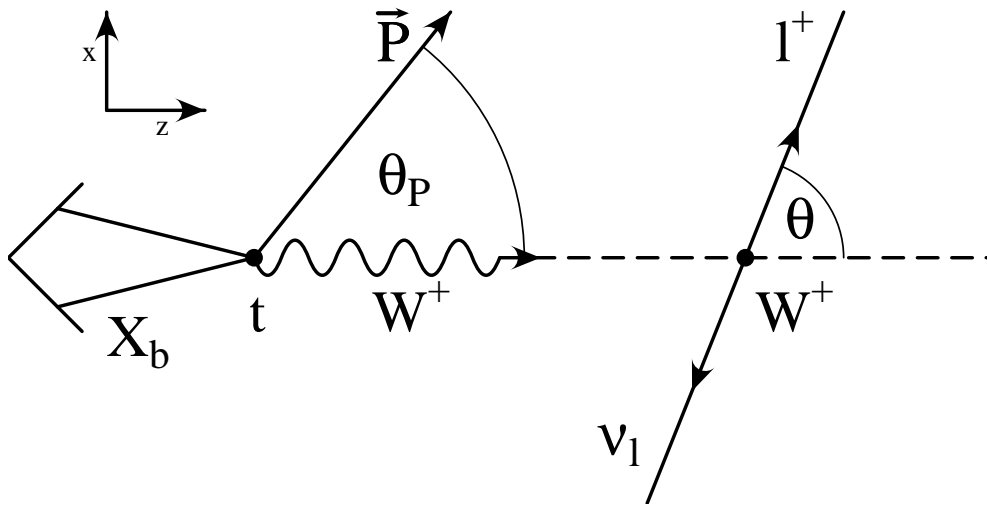


Figure 3